JACS
JOURNAL OF THE AMERICAN CHEMICAL SOCIETY
pubs.acs.org/JACS
Communication

Detection of Water Molecules on the Radical Transfer Pathway of Ribonucleotide Reductase by ^{17}O Electron−Nuclear Double Resonance Spectroscopy

Fabian Hecker, JoAnne Stubbe, and Marina Bennati*

Cite This: J. Am. Chem. Soc. 2021, 143, 7237−7241
Read Online
ACCESS | Metrics & More | Article Recommendations | Supporting Information

ABSTRACT: The role of water in biological proton-coupled electron transfer (PCET) is emerging as a key for understanding mechanistic details at atomic resolution. Here we demonstrate ^{17}O high-frequency electron−nuclear double resonance (ENDOR) in conjunction with $H_2{}^{17}O$-labeled protein buffer to establish the presence of ordered water molecules at three radical intermediates in an active enzyme complex, the $\alpha_2\beta_2$ *E. coli* ribonucleotide reductase. Our data give unambiguous evidence that all three, individually trapped, intermediates are hyperfine coupled to one water molecule with Tyr-O···^{17}O distances in the range 2.8−3.1 Å. The availability of this structural information will allow for quantitative models of PCET in this prototype enzyme. The results also provide a spectroscopic signature for water H-bonded to a tyrosyl radical.

Water is no longer known as just the solvent in which biochemical reactions take place but has been recognized as an essential player in these reactions.[1] Of particular interest is water involvement in electron transfer processes,[2−5] its action as a proton wire[6−8] or its role in proton-coupled electron transfer (PCET).[9−12] The identification of internal water in proteins can be achieved by X-ray diffraction.[13−15] However, the crystallization of transient protein complexes is difficult. One key approach for detection of water in biological systems has been the use of ^{17}O-enriched water in conjunction with magnetic resonance spectroscopy.[16−21] Among these methods, electron paramagnetic resonance (EPR) can take advantage of high selectivity, as it detects nuclei only in the ligand sphere ($r \lesssim 1.5$ nm)[22] of paramagnetic centers.

EPR-based ^{17}O hyperfine (hf) spectroscopy has been established for the detection of water binding to transition-metal ions, where the oxygen usually coordinates to the ion and large hyperfine couplings (several MHz) can be observed.[23−25] However, the most common water coordination motif to biological radicals occurs via H-bond interactions. The hf coupling to ^{17}O is diminished in comparison to the metal ion coordination, due to a longer interspin distance. In addition, the small ^{17}O gyromagnetic ratio ($\gamma_H/\gamma_{^{17}O} \approx 7.4$)[26] and high nuclear spin ($I = 5/2$) have rendered the ^{17}O hf coupling difficult to resolve.

Here we illustrate that high-frequency (94 and 263 GHz) electron−nuclear double resonance (ENDOR) spectroscopy can detect the ^{17}O signal of ordered water molecules at an H-bond distance to radical intermediates in *E. coli* ribonucleotide reductase (RNR). The enzyme uses a long-range (32 Å) radical transfer (RT) to initiate nucleotide reduction (Scheme 1).[27] Three tyrosines (Y_{356}, Y_{731}, and Y_{730}) are essential pathway residues, which form transient intermediates in the active complex $\alpha_2\beta_2$, consisting of the two homodimeric subunits α_2 and β_2.[13,27] Water has been observed only crystallographically in inactive α_2s without β_2.[13,14,28,29] Using site-selectively inserted tyrosine analogues to trap Y intermediates,[30] our previous $^1H/^2H$ ENDOR and DFT studies[10,11,31] revealed H-bonds attributed to water molecules and proposed a role of water in RT. However, all active sites of proteins have exchangeable protons, and thus alternative interpretations to our water proposal were possible. Recently, a cryo-EM structure of $\alpha_2\beta_2$ was reported but the resolution

Scheme 1. Current PCET Model of the 32 Å (Y_{122} to C_{439}) RT in *E. coli* RNR[27,32,a]

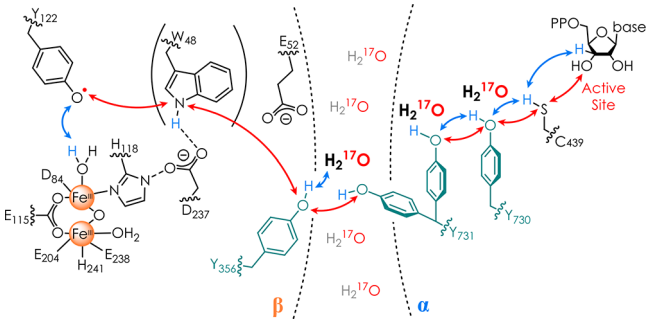

[a]Redox-active tyrosines 356, 731, and 730 are shown in cyan, electron transfer steps as red arrows, and proton transfer steps as blue arrows. Water molecules revealed in this study in respective site-selective mutants are shown in boldface.

Received: February 3, 2021
Published: May 6, 2021

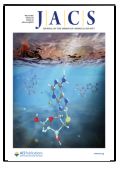

https://doi.org/10.1021/jacs.1c01359
J. Am. Chem. Soc. 2021, 143, 7237−7241

was insufficient for water observation.[32] Since our original proposals, studies using photo-RNRs and MD simulations implying waters in $\alpha_2\beta_2$ have appeared.[33,34] However, water has never been directly detected.

Therefore, we explored the capability of $H_2{}^{17}O$ ENDOR spectroscopy by exchanging the RNR buffer with $H_2{}^{17}O$. $\alpha_2\beta_2$-$Y_{356}^{\bullet}$ was generated by a 2,3,5-$F_3Y_{122}^{\bullet}$ mutation in β_2,[35] whereas radicals at Y_{731} and Y_{730} were trapped by replacing the respective residue with 3-aminotyrosine (NH_2Y),[36] leading to $\alpha_2\beta_2$-$NH_2Y_{731}^{\bullet}$ and $\alpha_2\beta_2$-$NH_2Y_{730}^{\bullet}$. The individual variants were mixed with the complementary α_2 or β_2 protein, CDP as a substrate, and ATP as an effector. The reaction was then quenched after a few seconds inside EPR tubes. Details on the sample preparation are given in sections SI1 and SI2.

Figure 1 displays representative 94 GHz ^{17}O Mims[37] ENDOR spectra of the radical intermediates.

Each spectrum shows a sharp doublet centered on the ^{17}O Larmor frequency (19.3 MHz at 3.4 T), which can be assigned to the central spin transition ($m_I(^{17}O) = +1/2 \rightarrow -1/2$) of one coupled ^{17}O nucleus. As ^{17}O is contained only in the water of the protein buffer, these sharp signals must arise from water molecules coupled to the radicals. Control experiments with only β_2 protein confirmed that the signal is associated to the radicals generated in $\alpha_2\beta_2$ (section SI3). The broad resonances at ±2.5 MHz are attributed to other nuclear transitions of the $I = 5/2$ spin system, broadened by nuclear quadrupole coupling (Figure 1A). Additionally, we note asymmetry of the doublet, which arises from second-order effects of the quadrupole coupling (section SI4). A comparison of the ENDOR spectra at the low ($B_0 \| g_x$) and high-field ($B_0 \| g_z$) edges of the EPR line (section SI5) indicates an almost isotropic hf coupling, with the dipolar contribution dominating the line width of the central doublet. The ^{17}O ENDOR spectra could be simulated with one ^{17}O nucleus, from which the asymmetry of the central peaks resulted using full diagonalization of the spin Hamiltonian (Figure 1 and section SI8). Parameters are given in Table 1 and section SI3. The spectra of $Y_{356}^{\bullet}$ and $NH_2Y_{731}^{\bullet}$ additionally contain signals close to the Larmor frequency not reproduced in the simulations, which likely originate from second-sphere water molecules at the subunit interface. Additional broadening is also observed, particularly at $NH_2Y_{731}^{\bullet}$. It might be caused by conformational distribution of this residue, which was found to have flexibility.[39,40,33]

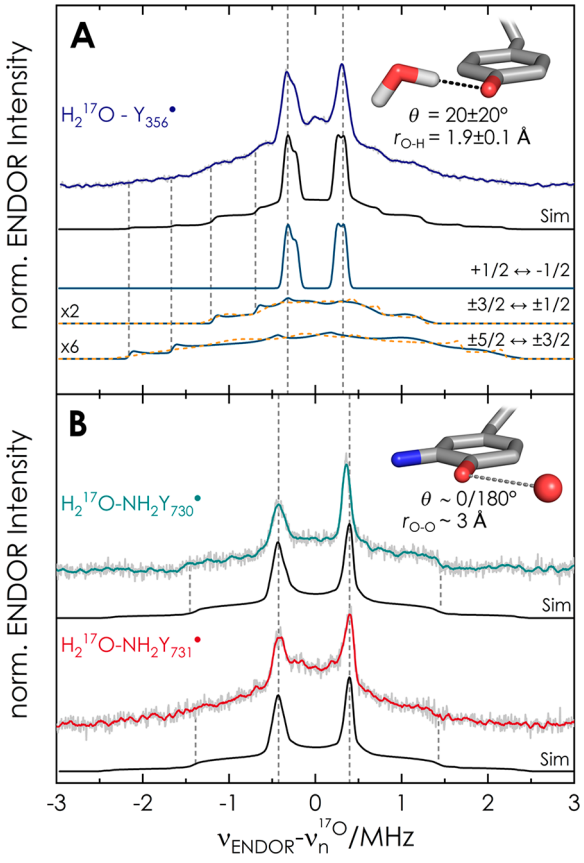

Figure 1. 94 GHz ^{17}O Mims[37] ENDOR spectra of (A) the intermediate $Y_{356}^{\bullet}$ and (B) $NH_2Y_{731}^{\bullet}$ and $NH_2Y_{730}^{\bullet}$ at $B_0 \| g_y$ in the EPR line (T = 50 K, τ_{Mims} = 390 ns). Acquisition time: 46 h ($Y_{356}^{\bullet}$), 40 h ($NH_2Y_{731}^{\bullet}$), and 18 h ($NH_2Y_{730}^{\bullet}$). $Y_{356}^{\bullet}$ is from β_2-$F_3Y_{122}^{\bullet}/\alpha_2$-$Y_{730}F$, which gives the highest radical yield (section SI2). Experimental spectra are shown in gray, with a Savitzky−Golay filter (fourth-order polynomial, 20-point window) shown in color. Simulations used Easyspin[38] (section SI1.6) with parameters given in Table 1 and section S3. Solid lines (teal) represent transitions among $m_I > 0$ manifolds and dashed lines (orange) those among $m_I < 0$ manifolds. The simulation does not distinguish between dihedral $\theta = 0°$ or $\theta = 180°$.

Table 1. Simulation and DFT Parameters for ^{17}O and ^{1}H hf Couplings of Water in RNR Intermediates[a]

	$Y_{356}^{\bullet}$ sim/ DFT_{small}	$NH_2Y_{731}^{\bullet}$ sim	$NH_2Y_{730}^{\bullet}$ sim/ DFT_{large}[b]
A_x (^{17}O)	0.43/0.19	0.70	0.65/0.24
A_y (^{17}O)	0.66/0.59	0.84	0.80/0.6
A_z (^{17}O)	0.70/0.65	0.89	0.89/0.6
$A(H_1)$	6.2[31]/7.4	≲2.5[b]	2.7[b]/4.2
$\rho(^{17}O)$[c] (%)	0.05		0.03
$r_{O\cdots{}^{17}O}$ (Å)	2.9 ± 0.1	~3.0	~3.0

[a]Except as noted, values are in MHz. Simulated quadrupole values for ^{17}O were $\{P_x;P_y;P_z\} = \{-0.02;-0.32;0.34\}$ MHz with e^2qQ/h = 6.8 MHz and η = 0.93.[41] [b]Values from ^{2}H couplings in refs 11 and 10 using $\gamma^{1}_{H}/\gamma^{2}_{H} \approx 6.5$.[26] [c]Loewdin spin density[42] from DFT. Uncertainties in coupling constants are less than 10% for simulations and up to 20% for DFT.

To rationalize the coupling, we began with a DFT-optimized small model (25 atoms, details in section SI1) of $Y_{356}^{\bullet}$, as previous ENDOR spectra revealed ^{1}H couplings consistent with one water at the H-bond distance $r_{O-H} \approx 1.8$ Å.[31] The ^{17}O coupling from this model was $A_{max}(^{17}O) \approx 1$ MHz, slightly exceeding the present experimental value of 0.6 ± 0.05 MHz. To optimize the model, we computed dihedral θ ($C_3-C_4-O\cdots H$) and distance scans for ^{17}O couplings, including the quadrupole tensor and the relative energies (section SI6). The DFT equilibrium distance always resulted in $r_{O-H} \approx 1.8$ Å. We found that hf couplings and energies vary significantly with θ, while the quadrupole coupling is less affected (Figure S9A−C). A_{xyz} values of ≲1 MHz are found for θ in the range ≲±30° (or equivalently 150° ≲ θ ≲ 240°): i.e., close to the ring plane. Water coordination in the ring plane also results in minimal relative energies (Figure S9B). Importantly, predicted spin densities on ^{17}O are <0.1% but are sufficient for producing a marked ^{17}O isotropic splitting. The spin density transfer or spin polarization is likely related to the H-bond nature. A distance scan for the optimized dihedral of +20° predicts $A_{max}(^{17}O)$ in the range 0.75−0.56 MHz (Figure S10A) for

https://doi.org/10.1021/jacs.1c01359
J. Am. Chem. Soc. 2021, 143, 7237−7241

$r_{O-H} \approx 1.8-2.0$ Å. Consideration of the DFT-predicted ^{1}H couplings (Figure S10B) and comparison with the experimental values[31] of ~6.2 (H_1) and ~1.6 MHz (H_2) indicates that the water is located at $r_{Tyr\text{-}O\cdots^{17}O} = 2.9 \pm 0.1$ Å, corresponding to an r_{O-H} value of 1.9 ± 0.1 Å. Notably, the DFT-predicted dipolar coupling ($T_{\parallel} \approx 0.3$ MHz, section SI6) is consistent with the point-dipole model and the aforementioned broadening of the sharp peaks.

Analogous DFT calculations were performed on the isolated amino tyrosyl $NH_2Y^{\bullet}$.[10,11,36] We observed a trend for the ^{17}O hf coupling in the dihedral and distance scans (section SI7) very similar to the $Y^{\bullet}$ model. The calculation predicts that $A_{iso}(^{17}O)$ of $NH_2Y^{\bullet}$ is slightly larger (10−15%) than that of $Y^{\bullet}$ at similar Tyr-O···^{17}O distances and orientations, which could explain the experimental observation. The amino group introduces an asymmetry in the radical, and the energetically most favored water orientation is found at the opposite side of the amino group (Figure S11B). Nevertheless, this small model could not account simultaneously for the ^{17}O and ^{1}H couplings observed for these two intermediates (Figure S12). As noted in a previous g_x calculation,[10] the coordination of the water molecule to $NH_2Y^{\bullet}$s is influenced by the surrounding second-sphere residues, as these two intermediates are buried in $\alpha_2\beta_2$ (Scheme 1).

Having established that at least one water molecule is hf-coupled to each of the three intermediates, we examine their current molecular models in light of this finding. First, we consider the radical site $Y_{356}^{\bullet}$ (Scheme 1). To explain the unprecedented g_x value of $Y_{356}^{\bullet}$ ($g_x = 2.0062$), we previously proposed that two almost equivalent waters might be simultaneously bonded to $Y_{356}^{\bullet}$.[31] While the present results are most consistent with the distance and orientation proposed for one water, the 94 GHz ^{17}O ENDOR spectra (Figure 1A) cannot resolve a second water. We note that the spectral line shape and ^{17}O hf coupling in Figure 1A are conserved in other RNR constructs that generate $Y_{356}^{\bullet}$ (section SI8), including the $F_3Y_{122}^{\bullet}/E_{52}Q\text{-}\beta_2$ double mutant used to solve a recent cryo-EM structure.[43]

To gain spectral resolution, we recorded ^{17}O ENDOR spectra of $Y_{356}^{\bullet}$ at 263 GHz/9.4 T (Figure 2).[44−46]

The results illustrate that the line width of the central doublet substantially narrows, particularly at $B_0 \| g_z$ (Figure 2). Despite the narrowing, a factor of approximately 2 from 94 to 263 GHz, we cannot discern two distinct ^{17}O contributions. Simulations of the 263 GHz spectra with the same parameters used at 94 GHz reproduce the line narrowing and support the analysis at 94 GHz. The lack of evidence for a second, almost equivalent water H-bonded to $Y_{356}^{\bullet}$ strongly suggests that the two-water model has become very unlikely and alternative explanations for the shifted g_x value of $Y_{356}^{\bullet}$ will have to be examined. The precise location of second-sphere residues might play a role,[12] which will require further experimental and computational investigation.

For the radical intermediates in the subunit α, a previous combined ENDOR/DFT model of $NH_2Y_{730}^{\bullet}$ proposed a water molecule coordinated in plane at a distance $r_{NH_2Y_{730}\text{-}O\cdots^{17}O} \approx 3.0$ Å.[10] The present results are consistent with this model and provide direct evidence for this postulated water in the enzyme complex $\alpha_2\beta_2\text{-}NH_2Y_{730}^{\bullet}$. The DFT-predicted hf parameters (DFT_{large}) for this large model (140 atoms) are reported in Table 1, and the model is displayed in section SI9.

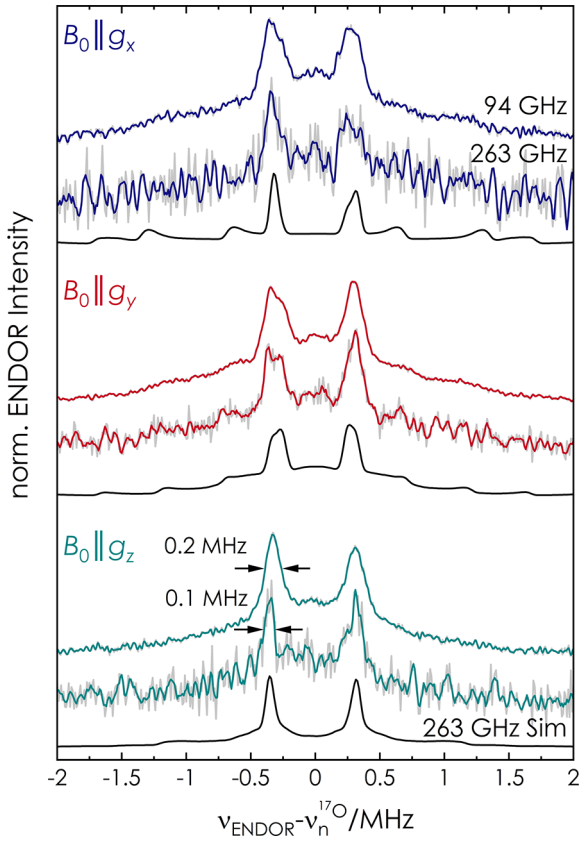

Figure 2. Comparison of 94 and 263 GHz Mims ENDOR of $Y_{356}^{\bullet}$ at the three canonical positions in the EPR line. Total acquisition time for 263 GHz (T = 20 K): 18 h ($B_0 \| g_x$), 10 h ($B_0 \| g_y$), and 11 h ($B_0 \| g_z$). Experimental spectra are shown in gray, with a Savitzky−Golay filter (fourth-order polynomial, 10 point window) in color. Simulations of 263 GHz spectra are in black with parameters as for 94 GHz (see Table 1 and Table S4).

Finally, for $\alpha_2\beta_2\text{-}NH_2Y_{731}^{\bullet}$, large-scale (215 atoms) DFT calculations previously proposed three models of the trapped intermediate (section SI10). Among these models, only one (model 3, Figure S15) contained a water molecule at an H-bond distance. The DFT-predicted ^{17}O hf couplings of model 3 (~2.5 MHz), however, largely exceed the present experimental values (Table S5). However, this DFT model did not include residues from the β subunit, which we now know are close to this residue in the active complex.[43] Therefore, the model will require further refinement. Nevertheless, the present results give evidence for a water molecule coordinated almost in the plane of $NH_2Y_{731}^{\bullet}$.

In conclusion, we have reported the capability of ^{17}O high-frequency ENDOR to detect water H-bonded to tyrosyl radicals. The spectroscopic approach led to the first detection of ordered water molecules at three trapped radicals proposed to be representative of $Y^{\bullet}$ intermediates in the PCET of *E. coli* RNR. These results verify previous hypotheses on the presence and role of water in the RNR mechanism and provide a new starting point for computational studies. Knowledge of this ^{17}O signature will also be generally useful for many other biological systems, in which tyrosyl radicals are involved.

https://doi.org/10.1021/jacs.1c01359
J. Am. Chem. Soc. 2021, 143, 7237−7241

■ ASSOCIATED CONTENT

Supporting Information

The Supporting Information is available free of charge at https://pubs.acs.org/doi/10.1021/jacs.1c01359.

Experimental procedure, radical yield determination, ENDOR spectra of $Y_{122}^{\bullet}$ and $F_3Y_{122}^{\bullet}$, ENDOR spectra of $I = 5/2$ nuclei, orientation-selective ENDOR spectra, DFT models of $Y^{\bullet}$ and $NH_2Y^{\bullet}$, ^{17}O $Y_{356}^{\bullet}$ spectra of different mutants, previous large DFT models of $\alpha_2\beta_2$-$NH_2Y_{730}^{\bullet}$ and $\alpha_2\beta_2$-$NH_2Y_{731}^{\bullet}$ (PDF)

■ AUTHOR INFORMATION

Corresponding Author

Marina Bennati − *Max Planck Institute for Biophysical Chemistry, 37077 Göttingen, Germany; Department of Chemistry, Georg-August-University, 37077 Göttingen, Germany;* orcid.org/0000-0001-6784-7845; Email: marina.bennati@mpibpc.mpg.de

Authors

Fabian Hecker − *Max Planck Institute for Biophysical Chemistry, 37077 Göttingen, Germany*

JoAnne Stubbe − *Department of Chemistry, Massachusetts Institute of Technology, Cambridge, Massachusetts 20139, United States;* orcid.org/0000-0001-8076-4489

Complete contact information is available at: https://pubs.acs.org/10.1021/jacs.1c01359

Funding

This work was funded by the Max Planck Society and the DFG priority program SPP1601 to M.B. as well as an NIH grant 29595 to J.S.

Notes

The authors declare no competing financial interest.

■ ACKNOWLEDGMENTS

We thank Brandon Greene (UCSB) for his help in producing protein samples in ^{17}O-labeled buffer. We also thank Markus Hiller (MPIBPC) for discussions about DFT modeling, Igor Tkach (MPIBPC) for assistance with instrumentation, and Andreas Meyer (MPIBPC) for discussions and suggestions.

■ REFERENCES

(1) Ball, P. Water as an active constituent in cell biology. *Chem. Rev.* **2008**, *108* (1), 74−108.

(2) Tezcan, F. A.; Crane, B. R.; Winkler, J. R.; Gray, H. B. Electron tunneling in protein crystals. *Proc. Natl. Acad. Sci. U. S. A.* **2001**, *98* (9), 5002−6.

(3) van Amsterdam, I. M.; Ubbink, M.; Einsle, O.; Messerschmidt, A.; Merli, A.; Cavazzini, D.; Rossi, G. L.; Canters, G. W. Dramatic modulation of electron transfer in protein complexes by crosslinking. *Nat. Struct. Biol.* **2002**, *9* (1), 48−52.

(4) Lin, J.; Balabin, I. A.; Beratan, D. N. The nature of aqueous tunneling pathways between electron-transfer proteins. *Science* **2005**, *310* (5752), 1311−1313.

(5) de la Lande, A.; Marti, S.; Parisel, O.; Moliner, V. Long distance electron-transfer mechanism in peptidylglycine alpha-hydroxylating monooxygenase: a perfect fitting for a water bridge. *J. Am. Chem. Soc.* **2007**, *129* (38), 11700−7.

(6) Luecke, H.; Schobert, B.; Richter, H. T.; Cartailler, J. P.; Lanyi, J. K. Structure of bacteriorhodopsin at 1.55 A resolution. *J. Mol. Biol.* **1999**, *291* (4), 899−911.

(7) Sass, H. J.; Buldt, G.; Gessenich, R.; Hehn, D.; Neff, D.; Schlesinger, R.; Berendzen, J.; Ormos, P. Structural alterations for proton translocation in the M state of wild-type bacteriorhodopsin. *Nature* **2000**, *406* (6796), 649−53.

(8) Linke, K.; Ho, F. M. Water in Photosystem II: structural, functional and mechanistic considerations. *Biochim. Biophys. Acta, Bioenerg.* **2014**, *1837* (1), 14−32.

(9) Saito, K.; Shen, J. R.; Ishida, T.; Ishikita, H. Short hydrogen bond between redox-active tyrosine Y(Z) and D1-His190 in the photosystem II crystal structure. *Biochemistry* **2011**, *50* (45), 9836−44.

(10) Argirevic, T.; Riplinger, C.; Stubbe, J.; Neese, F.; Bennati, M. ENDOR spectroscopy and DFT calculations: evidence for the hydrogen-bond network within α2 in the PCET of E. coli ribonucleotide reductase. *J. Am. Chem. Soc.* **2012**, *134* (42), 17661−70.

(11) Nick, T. U.; Lee, W.; Kossmann, S.; Neese, F.; Stubbe, J.; Bennati, M. Hydrogen bond network between amino acid radical intermediates on the proton-coupled electron transfer pathway of E. coli α2 ribonucleotide reductase. *J. Am. Chem. Soc.* **2015**, *137* (1), 289−98.

(12) Sirohiwal, A.; Neese, F.; Pantazis, D. A. Microsolvation of the Redox-Active Tyrosine-D in Photosystem II: Correlation of Energetics with EPR Spectroscopy and Oxidation-Induced Proton Transfer. *J. Am. Chem. Soc.* **2019**, *141* (7), 3217−3231.

(13) Uhlin, U.; Eklund, H. Structure of ribonucleotide reductase protein R1. *Nature* **1994**, *370* (6490), 533−9.

(14) Eriksson, M.; Uhlin, U.; Ramaswamy, S.; Ekberg, M.; Regnström, K.; Sjöberg, B.-M.; Eklund, H. Binding of allosteric effectors to ribonucleotide reductase protein R1: reduction of active-site cysteines promotes substrate binding. *Structure* **1997**, *5* (8), 1077−1092.

(15) Umena, Y.; Kawakami, K.; Shen, J. R.; Kamiya, N. Crystal structure of oxygen-evolving photosystem II at a resolution of 1.9 A. *Nature* **2011**, *473* (7345), 55−60.

(16) Schmidt, B.; McCracken, J.; Ferguson-Miller, S. A discrete water exit pathway in the membrane protein cytochrome c oxidase. *Proc. Natl. Acad. Sci. U. S. A.* **2003**, *100* (26), 15539−42.

(17) Bennati, M.; Hertel, M. M.; Fritscher, J.; Prisner, T. F.; Weiden, N.; Hofweber, R.; Sporner, M.; Horn, G.; Kalbitzer, H. R. High-frequency 94 GHz ENDOR characterization of the metal binding site in wild-type Ras x GDP and its oncogenic mutant G12V in frozen solution. *Biochemistry* **2006**, *45* (1), 42−50.

(18) Potapov, A.; Goldfarb, D. The Mn(2+)-bicarbonate complex in a frozen solution revisited by pulse W-band ENDOR. *Inorg. Chem.* **2008**, *47* (22), 10491−8.

(19) McConnell, I. L.; Grigoryants, V. M.; Scholes, C. P.; Myers, W. K.; Chen, P. Y.; Whittaker, J. W.; Brudvig, G. W. EPR-ENDOR characterization of (^{17}O, ^{1}H, ^{2}H) water in manganese catalase and its relevance to the oxygen-evolving complex of photosystem II. *J. Am. Chem. Soc.* **2012**, *134* (3), 1504−12.

(20) Nalepa, A.; Malferrari, M.; Lubitz, W.; Venturoli, G.; Mobius, K.; Savitsky, A. Local water sensing: water exchange in bacterial photosynthetic reaction centers embedded in a trehalose glass studied using multiresonance EPR. *Phys. Chem. Chem. Phys.* **2017**, *19* (41), 28388−28400.

(21) Rowlands, L. J.; Marks, A.; Sanderson, J. M.; Law, R. V. ^{17}O NMR spectroscopy as a tool to study hydrogen bonding of cholesterol in lipid bilayers. *Chem. Commun.* **2020**, *56* (92), 14499−14502.

(22) Meyer, A.; Dechert, S.; Dey, S.; Hobartner, C.; Bennati, M. Measurement of Angstrom to Nanometer Molecular Distances with ^{19}F Nuclear Spins by EPR/ENDOR Spectroscopy. *Angew. Chem., Int. Ed.* **2020**, *59* (1), 373−379.

(23) Raitsimring, A. M.; Astashkin, A. V.; Baute, D.; Goldfarb, D.; Caravan, P. W-Band ^{17}O Pulsed Electron-Nuclear Double Resonance Study of Gadolinium Complexes with Water. *J. Phys. Chem. A* **2004**, *108* (35), 7318−7323.

(24) Baute, D.; Goldfarb, D. The 17O hyperfine interaction in $V^{17}O(H_2{}^{17}O)^{52+}$ and $Mn(H_2{}^{17}O)^{62+}$ determined by high field

ENDOR aided by DFT calculations. *J. Phys. Chem. A* **2005**, *109* (35), 7865−71.
(25) Rapatskiy, L.; Cox, N.; Savitsky, A.; Ames, W. M.; Sander, J.; Nowaczyk, M. M.; Rogner, M.; Boussac, A.; Neese, F.; Messinger, J.; Lubitz, W. Detection of the water-binding sites of the oxygen-evolving complex of Photosystem II using W-band ^{17}O electron-electron double resonance-detected NMR spectroscopy. *J. Am. Chem. Soc.* **2012**, *134* (40), 16619−34.
(26) Tiesinga, E.; Mohr, P. J.; Newell, D. B.; Taylor, B. N. *CODATA Recommended Values of the Fundamental Physical Constants: 2018*; https://physics.nist.gov/cuu/Constants/index.html (accessed 2021-01-15).
(27) Greene, B. L.; Kang, G.; Cui, C.; Bennati, M.; Nocera, D. G.; Drennan, C. L.; Stubbe, J. Ribonucleotide Reductases: Structure, Chemistry, and Metabolism Suggest New Therapeutic Targets. *Annu. Rev. Biochem.* **2020**, *89*, 45−75.
(28) Yokoyama, K.; Uhlin, U.; Stubbe, J. Site-specific incorporation of 3-nitrotyrosine as a probe of pKa perturbation of redox-active tyrosines in ribonucleotide reductase. *J. Am. Chem. Soc.* **2010**, *132* (24), 8385−97.
(29) Minnihan, E. C.; Seyedsayamdost, M. R.; Uhlin, U.; Stubbe, J. Kinetics of radical intermediate formation and deoxynucleotide production in 3-aminotyrosine-substituted Escherichia coli ribonucleotide reductases. *J. Am. Chem. Soc.* **2011**, *133* (24), 9430−40.
(30) Minnihan, E. C.; Nocera, D. G.; Stubbe, J. Reversible, long-range radical transfer in E. coli class Ia ribonucleotide reductase. *Acc. Chem. Res.* **2013**, *46* (11), 2524−35.
(31) Nick, T. U.; Ravichandran, K. R.; Stubbe, J.; Kasanmascheff, M.; Bennati, M. Spectroscopic Evidence for a H Bond Network at Y_{356} Located at the Subunit Interface of Active E. coli Ribonucleotide Reductase. *Biochemistry* **2017**, *56* (28), 3647−3656.
(32) Kang, G.; Taguchi, A. T.; Stubbe, J.; Drennan, C. L. Structure of a trapped radical transfer pathway within a ribonucleotide reductase holocomplex. *Science* **2020**, *368* (6489), 424−427.
(33) Reinhardt, C. R.; Li, P.; Kang, G.; Stubbe, J.; Drennan, C. L.; Hammes-Schiffer, S. Conformational Motions and Water Networks at the alpha/beta Interface in E. coli Ribonucleotide Reductase. *J. Am. Chem. Soc.* **2020**, *142* (32), 13768−13778.
(34) Cui, C.; Greene, B. L.; Kang, G.; Drennan, C. L.; Stubbe, J.; Nocera, D. G. Gated Proton Release during Radical Transfer at the Subunit Interface of Ribonucleotide Reductase. *J. Am. Chem. Soc.* **2021**, *143* (1), 176−183.
(35) Minnihan, E. C.; Young, D. D.; Schultz, P. G.; Stubbe, J. Incorporation of fluorotyrosines into ribonucleotide reductase using an evolved, polyspecific aminoacyl-tRNA synthetase. *J. Am. Chem. Soc.* **2011**, *133* (40), 15942−5.
(36) Lee, W.; Kasanmascheff, M.; Huynh, M.; Quartararo, A.; Costentin, C.; Bejenke, I.; Nocera, D. G.; Bennati, M.; Tommos, C.; Stubbe, J. Properties of Site-Specifically Incorporated 3-Aminotyrosine in Proteins To Study Redox-Active Tyrosines: Escherichia coli Ribonucleotide Reductase as a Paradigm. *Biochemistry* **2018**, *57* (24), 3402−3415.
(37) Mims, W. B. Pulsed endor experiments. *Proc. R. Soc. London, Ser. A* **1965**, *283* (1395), 452−457.
(38) Stoll, S.; Schweiger, A. EasySpin, a comprehensive software package for spectral simulation and analysis in EPR. *J. Magn. Reson.* **2006**, *178* (1), 42−55.
(39) Kasanmascheff, M.; Lee, W.; Nick, T. U.; Stubbe, J.; Bennati, M. Radical transfer in E. coli ribonucleotide reductase: a NH_2Y_{731}/R411A-α mutant unmasks a new conformation of the pathway residue 731. *Chem. Sci.* **2016**, *7* (3), 2170−2178.
(40) Greene, B. L.; Taguchi, A. T.; Stubbe, J.; Nocera, D. G. Conformationally Dynamic Radical Transfer within Ribonucleotide Reductase. *J. Am. Chem. Soc.* **2017**, *139* (46), 16657−16665.
(41) Edmonds, D. T.; Zussman, A. Pure quadrupole resonance of ^{17}O in ice. *Phys. Lett. A* **1972**, *41* (2), 167−169.
(42) Löwdin, P. O. On the Non-Orthogonality Problem Connected with the Use of Atomic Wave Functions in the Theory of Molecules and Crystals. *J. Chem. Phys.* **1950**, *18* (3), 365−375.
(43) Lin, Q.; Parker, M. J.; Taguchi, A. T.; Ravichandran, K.; Kim, A.; Kang, G.; Shao, J.; Drennan, C. L.; Stubbe, J. Glutamate 52-β at the α/β subunit interface of Escherichia coli class Ia ribonucleotide reductase is essential for conformational gating of radical transfer. *J. Biol. Chem.* **2017**, *292* (22), 9229−9239.
(44) Jakobsen, H. J.; Bildsøe, H.; Brorson, M.; Wu, G.; Gor'kov, P. L.; Gan, Z.; Hung, I. High-Field ^{17}O MAS NMR Reveals $^{1}J(^{17}O\text{-}^{127}I)$ with its Sign and the NMR Crystallography of the Scheelite Structures for $NaIO_4$ and KIO_4. *J. Phys. Chem. C* **2015**, *119* (25), 14434−14442.
(45) Keeler, E. G.; Michaelis, V. K.; Colvin, M. T.; Hung, I.; Gor'kov, P. L.; Cross, T. A.; Gan, Z.; Griffin, R. G. ^{17}O MAS NMR Correlation Spectroscopy at High Magnetic Fields. *J. Am. Chem. Soc.* **2017**, *139* (49), 17953−17963.
(46) Tkach, I.; Bejenke, I.; Hecker, F.; Kehl, A.; Kasanmascheff, M.; Gromov, I.; Prisecaru, I.; Hofer, P.; Hiller, M.; Bennati, M. ^{1}H high field electron-nuclear double resonance spectroscopy at 263 GHz/9.4T. *J. Magn. Reson.* **2019**, *303*, 17−27.

https://doi.org/10.1021/jacs.1c01359
J. Am. Chem. Soc. 2021, 143, 7237−7241